International Journal of Biological Macromolecules 267 (2024) 131553

Contents lists available at ScienceDirect

International Journal of Biological Macromolecules

journal homepage: www.elsevier.com/locate/ijbiomac

Periodate oxidation of nanofibrillated cellulose films for active packaging applications

Julia Fernández-Santos, Cristina Valls, Oriol Cusola, M. Blanca Roncero *

CELBIOTECH_Paper Engineering Research Group, Universitat Politècnica de Catalunya_BarcelonaTech, 08222 Terrassa, Spain

ARTICLE INFO

Keywords:
Nanocellulose films
Periodate oxidation
Immobilization of laccases

ABSTRACT

An alternative packaging material based on cellulose that possesses excellent barrier properties and is potentially useful for active packaging has been developed. Cellulose nanofibril was efficiently and selectively oxidized with sodium periodate generating reactive aldehyde groups. These groups formed hemiacetal and hemialdal bonds during film formation and, consequently, highly transparent, elastic and strong films were created even under moisture saturation conditions. The periodate oxidation treatment additionally decreased the polarity of the films and considerably enhanced their water barrier properties. Thus, the water contact angle of films treated for 3 and 6 h was 97° and 102°, their water drop test value was higher than in untreated film (viz., 138 and 141 min with 3 and 6 h of treatment) and their water vapour transmission rate was substantially better (3.31 and 0.78 g m^{-2} day^{-1} with 3 and 6 h, respectively). The presence of aldehyde groups facilitated immobilization of the enzyme laccase, which efficiently captures oxygen and prevents food decay as a result. Laccase-containing films oxidized 80 % of Methylene Blue colorant and retained their enzymatic activity after storage for 1 month and 12 reuse cycles, opening the door to the possible creation of a reusable packaging to replace the single-use packaging.

1. Introduction

The search for alternative materials intended to replace plastics in a number of fields has grown markedly over the last few decades. Cellulose is one of the most abundant natural polymers and possesses attractive properties that have elicited widespread studies on its potential use in the papermaking, textile, food and pharmaceutical industries, among others [1,2]. The presence of many hydroxyl groups in its structure makes it easy to modify for chemical conversion into a variety of biomaterials [3]. Worth special note in this respect is its conversion into nanocellulose [4], which possesses promising properties for use in nanocomposites and packaging applications [5,6]. In fact, nanocellulose retains some key properties of cellulose such as hydrophilicity and crystallinity, and additionally possesses a high specific surface area and optical transparency [6]. Nanocellulose can be obtained from plants, bacteria or tunicates, but is largely produced from wood or non-wood plant fibres (cotton, kenaf and wheat, mainly) [7,8].

The specific properties of nanocellulose vary slightly with its origin. Nanocellulose in plants is usually present in the form of nanocrystals (nanocrystalline cellulose, CNC) or nanofibres (cellulose nanofibril, CNF). CNC can be extracted by acid hydrolysis of the amorphous portion of nanocellulose, which provides a crystalline product [9,10]. On the other hand, CNF, which possesses a high specific surface area (fibres are typically 1–10 μm long and 10–100 nm thick), is usually obtained by high-shearing mechanical grinding of enzymatically or chemically pretreated cellulose fibres, and contains both crystalline and amorphous cellulose [11,12].

Because CNC is more crystalline than CNF, films obtained from the former are usually much more brittle and difficult to handle. Fernández-Santos et al. [13] found the relatively poor mechanical and barrier properties of CNC to be improved by some plasticizers. By contrast, CNF is easier to handle, and has very good mechanical and oxygen barrier properties. Such properties, however, are impaired by highly moist conditions [14]. Also, CNF films are less transparent than CNC films [15]. These shortcomings of CNF films can be circumvented by using various functionalization methods to introduce carbonyl or carboxyl

Abbreviations: CNC, cellulose nanocrystals; CNF, cellulose nanofibril; CNF ox., oxidized cellulose nanofibril; RH, relative humidity; WCA, water contact angle; WDT, water drop test; OP, oxygen permeability; WVTR, water vapour transmission rate; MB, Methylene Blue.

* Corresponding author.
E-mail addresses: julia.fernandez.santos@upc.edu (J. Fernández-Santos), cristina.valls@upc.edu (C. Valls), oriol.cusola@upc.edu (O. Cusola), blanca.roncero@upc.edu (M.B. Roncero).

https://doi.org/10.1016/j.ijbiomac.2024.131553
Received 20 February 2024; Received in revised form 5 April 2024; Accepted 10 April 2024
Available online 15 April 2024

groups in the nanocellulose structure [16,17]. Cellulose can be functionalized with aldehyde groups by using non-selective reagents such as nitrogen oxides, ozone or peroxides, or selective reagents such as periodate and nitroxyl radicals such as TEMPO (2,2,6,6-tetramethylpiperidine-*N*-oxyl) [18]. Periodate is an especially effective reagent for functionalizing nanocellulose by virtue of its high oxidation efficiency and selectivity [19]. Also, it affords stereospecific oxidation of the C_2-C_3 bond in the glucopyranose unit of glucose to two aldehyde groups per glucose unit [i.e., to dialdehyde cellulose (DAC)] [20,21]. Aldehyde groups thus formed can interact with one another, and also with hydroxyl groups in cellulose, to form hemiacetal bonds, which are especially useful for producing packaging materials with a high moisture resistance [16,22]. In addition, the presence of aldehyde groups allows biomaterials to adsorb heavy metals, drugs and proteins [23].

Decay in packaged food can alter its texture, nutritional properties and taste, and make it unacceptable for consumers as a result [24,25]. Food deterioration is caused mainly by bacteria, yeasts and mould, but can also be of chemical origin [26]. Minimizing the largely oxidative reactions involved requires using a material capable of capturing oxygen in the package (viz., one such as powdered iron or ascorbic acid to adsorb the oxygen [27], or a more innovative solution such as an oxygen-capturing enzyme [28]). Some oxidoreductases including laccases can efficiently capture oxygen in active packages. The high substrate specificity of these enzymes, which are produced by fungi, higher plants, bacteria, insects, lichens and sponges [29], has promoted their use in various biotechnological and industrial fields such as silviculture [30], food production [28], pulp and paper making [31], bioremediation [32], organic synthesis [33] and active packaging [28].

Laccases catalyse the oxidation of various substrates, but mainly phenolic compounds, while simultaneously reducing molecular oxygen to water. Therefore, they are potentially good candidates for reducing the oxygen concentration inside food packages. Effectively immobilizing an enzyme onto a support requires using an appropriate carrier and immobilization method [34] such as entrapment, encapsulation, adsorption, covalent binding or self-immobilization [35]. Agar, alginate and modified cellulose are the preferential supports for immobilizing laccases [36]. Aldehyde groups are known to exhibit a high affinity for amines in enzymes, so they can probably facilitate their immobilization [37] to produce functional bioactive biopackages.

In this work, we obtained an active biopackaging material by immobilizing laccase onto films of periodate-oxidized cellulose nanofibril (CNF). The films were characterized in terms of mechanical (elongation and tensile strength), barrier (air, water, fat, water vapour and oxygen) and optical properties. Additional determinations included assessing the effect of the oxidation treatment on the antioxidant capacity of the films. Chemical changes were examined by Fourier transform infrared (FTIR) spectroscopy, and internal and surface changes by scanning electron microscopy (SEM). Periodate-oxidized CNF films were used to immobilize laccase under optimal conditions and the immobilized enzyme was analysed for storage stability, reusability and reactivity to Methylene Blue.

2. Materials and methods

2.1. Materials

The main raw material used was cellulose nanofibril (CNF) supplied by the University of Maine (Orono, ME, USA). Sodium periodate ($NaIO_4$) was purchased from Merck (Darmstadt, Germany), 3-ethyl-benzothiazoline-6-sulphonic acid (ABTS) and Tween 20 (a polysorbate-type nonionic surfactant) were obtained from Sigma–Aldrich (St Louis, MO, USA), ethylene glycol was supplied by Panreac Química S.A.U. (Barcelona, Spain) and laccase by Novozymes Biopharma Co., Ltd. (Tianjin, China).

2.2. Oxidation of CNF with periodate

CNF films were prepared by casting, using the amount of water needed to obtain a final consistency of 2 % to commercial CNF under vigorous stirring at 700 rpm for 1 h. The resulting suspensions were deposited onto a polystyrene plastic surface and allowed to evaporate at a controlled relative humidity (50 %) and temperature (23 °C) for about 5 days.

A 0.5 M sodium periodate solution was prepared and carefully wrapped in aluminium foil to prevent light-induced decomposition. The solution was reacted with the previously obtained CNF films for 0 to 360 min. For this purpose, the films were placed in a tray and covered with periodate solution. No resistance to wetting was observed, i.e. the CNF film could be completely immersed and impregnated with the sodium periodate solution. The reaction was stopped by adding 5 mL of ethylene glycol and the films, once dry, were washed with distilled water to remove excess periodate.

2.3. Quantification of aldehyde groups

Aldehyde groups in the oxidized films were quantified by using the method of Pommerening [20,38], which is based on the Cannizzaro reaction and involves deprotonation of an aldehyde with a strong base such as NaOH to obtain and acid and an alcohol. The procedure involved placing small (5 mg) pieces of film in a beaker containing 5 mL of 10 mM NaOH at 70 °C and stirring for 15 min, followed by titration with 5 mM HCl. The concentration of aldehyde groups was calculated by using a slightly modified version of Pommerening's equation [20]:

$$\mu\text{mol aldehyde groups/mL} = [\text{mL NaOH} - \text{mL HCl}]/5 \quad (1)$$

2.4. Characterization of oxidized films

2.4.1. Structural properties

Film thickness, basis weight and density were measured according to ISO 534:2011, and roughness according to ISO 8791-2:2013. Paper surface area measurements were made with a ruler. Percent miniaturization was taken to be the decrease in oxidized film area relative to the unoxidized film. Film surfaces and cross-sections were viewed under a Hitachi SU1510 scanning electron microscope following gold-coated with Bio-Rad SC502 SEM coating system.

2.4.2. Optical properties

Film absorbance at room temperature was measured over the range 200–900 nm in 1 nm steps, using an Evolution 600 UV–visible spectrophotometer. Transmittance was measured at 600 nm, as it is the wavelength commonly used to calculate the film transparency [39–43] according to the following equation:

$$Transparency = (-log\%T_{600}/x) \quad (2)$$

where $\%T_{600}$ is the percent transmittance at 600 nm and x film thickness (mm).

2.4.3. Mechanical properties

Selected mechanical properties of the films such as tensile strength and elongation at break were determined under dry and wet conditions by using a Metrotect T5K quality control instrument from Techlab Systems (Lezo, Guipuzcoa, Spain) equipped with a 500 N load cell. The films were cut into rectangles 15 mm wide and 50 mm long for measurement. Tensile strength was assessed under both dry and wet conditions. In the wet tests, the samples were previously immersed in distilled water for 10 min and excess water was removed with filter paper. A wet/dry tensile strength ratio was calculated and expressed as a percentage.

2.4.4. Barrier properties

Air permeance was measured according to ISO 5636-3:2013, and water absorption was evaluated by using an adaptation of TAPPI T835 in which a drop of water was deposited onto the surface of the films and the time it took the specular gloss of the drop to disappear measured. Hydrophobicity was measured as the water contact angle (WCA), using an OCA15EC contact angle goniophotometer from Dataphysics Instruments GmbH (Filderstadt, Germany) at an image capture ratio of 25 frames s^{-1}. A 4 μL water drop was delivered to the sample surface to make at least 5 measurements per film (a total of 10 measurements per sample). Oil resistance was measured by using the turpentine test in accordance with ISO 16532-3:2010, and oxygen permeability with an OX-TRAN 1/50 gas analyser from Mocon (Brooklyn Park, MN, USA) at an atmospheric oxygen concentration of 100 % at 23 °C and a variable relative humidity (0, 20, 40, 60, 70, 80 or 90 %). The water vapour transmission rate (WVTR) of the films was determined at 25 °C at 50 % RH according to ISO 2528 (2017). The procedure was as follows: an aluminium cup containing $CaCl_2$ as desiccant was sealed with the test film (50 cm^2 film area) by using paraffin wax at 90 °C and placed in a climate chamber under controlled environmental conditions. All tests were performed in duplicate. WVTR (g m^{-2} day^{-1}) was calculated as follows:

$$WVTR = \left(m \times 24 \times 10^4\right)/(S \times t) \quad (3)$$

where m (g) is the increase in mass in the assembly during time t, S (cm^2) the area of the tested surface and t (h) the overall duration of the last two stable exposure periods.

2.4.5. FTIR spectroscopy

Duplicate FTIR spectra for the CNF films over the wavenumber range 500–4000 cm^{-1} were recorded at room temperature on a Spectrum 100 ATR-FTIR spectrophotometer from Perkin Elmer (Waltham, MA, USA). A total of 64 scans at 1 cm^{-1} resolution per spectrum were acquired.

2.4.6. Antioxidant capacity

The antioxidant capacity of the nanocomposite films was determined by using a modified version of the 2,2′-azinobis-(3-ethylbenzothiazoline-6-sulphonic acid) ($ABTS^{+\cdot}$) scavenging activity method of Valls and Roncero [4], and Cusola et al. (2015) [31]. The scavenging activity of the free radical was assessed spectrophotometrically by monitoring the disappearance of the absorption band at 752 nm for the free radical $ABTS^{+\cdot}$, which was obtained by oxidizing potassium persulphate and diluting the resulting solution to adjust the absorbance at 752 nm to 0.70 ± 0.1. For comparison, 10 mg amounts of nanocomposite film were added to 1.5 mL of $ABTS^{+\bullet}$ solutions and vortexed for about 2 min, followed by centrifugation at 6000 rpm for 4 min and storage at room temperature in the dark for 30 min prior to measuring the absorbance at 752 nm. The absorbance of the film-free control samples was also measured at 752 nm by following the same procedure. Antioxidant capacity was determined from at least 3 measurements per sample, using the following equation:

$$\text{Antioxidant activity } (\%) = [(A_0 - A_1)/A_0] \times 100 \quad (4)$$

where A_0 is the absorbance of the control sample and A_1 that of the nanocomposite film.

2.4.7. Surface free energy

Surface free energy (SFE) was determined by using the method of Owens, Wendt, Rabel and Kaelble (OWRK) [44]. Briefly, several drops of de-ionized water, ethylene glycol and di-iodomethane were applied to the surface of each sample before measuring the contact angle with a Dataphysics OCA15EC goniophotometer at an image capture ratio of 25 frames s^{-1}. At least 5 droplets of each liquid were dispensed in different regions of each sample. The total SFE of each sample was computed as the combination of polar and disperse contributions. The interfacial energy was calculated from the geometric mean of the contributions of the liquid and solid:

$$\sigma_l(1 + cos\theta) = 2\sqrt{\sigma_l^d \sigma_s^d} + 2\sqrt{\sigma_l^p \sigma_s^p} \quad (5)$$

where θ is the contact angle, σ_l the surface tension of the liquid, σ_l^d and σ_l^p denote the disperse and polar parts of the liquid, and σ_s^d and σ_s^p the respective contributions of the solid. Plotting Eq. (5) gave a straight line that allowed σ_s^p to be calculated from the slope and σ_s^d from the intercept. A minimum of 5 replicates per film sample were used to obtain an average value.

2.5. Immobilization of laccase

The procedure used to immobilize the enzyme was chosen with provision for the following potentially influential factors: (*a*) the use of water or a buffer as reaction medium; (*b*) the reaction temperature; (*c*) stirring; (*d*) the reaction time; and (e) the presence of a surfactant. The optimum procedure was found to involve adding a known amount of laccase solution to an Eppendorf flask containing CNF oxidized with periodate for 3 h and 0.2 mL of a polysorbate-type non-ionic surfactant, and allowing the mixture to stand unstirred at 4 °C for 1 h. The procedure was applied to wet films and to others previously dried for 3 h. After 1 h, the films containing immobilized laccase were washed with water for assessment of their enzyme activity. The tests on dry films

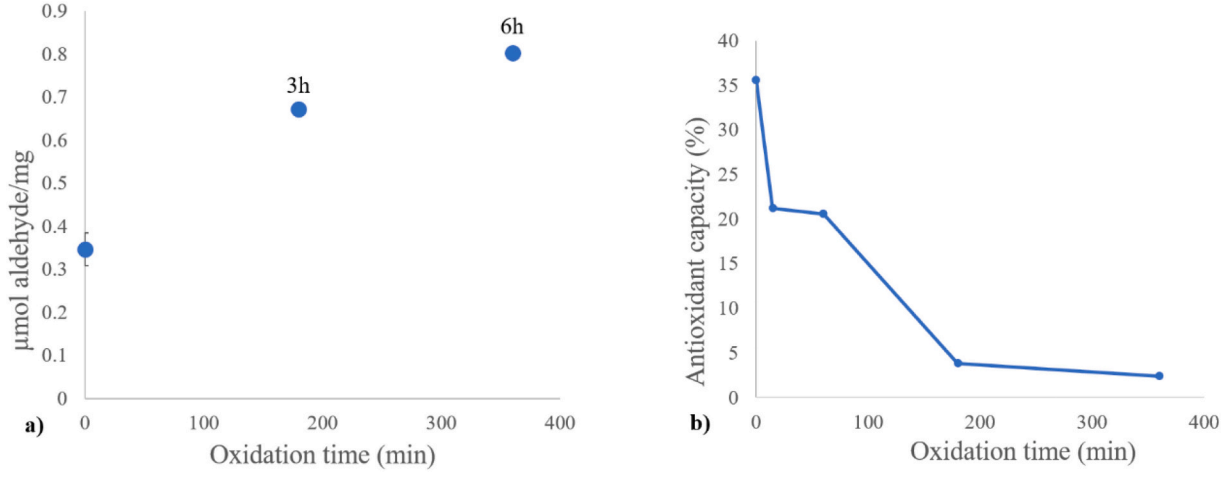

Fig. 1. a) Aldehyde content and b) antioxidant capacity of CNF films oxidized with periodate for variable lengths of time.

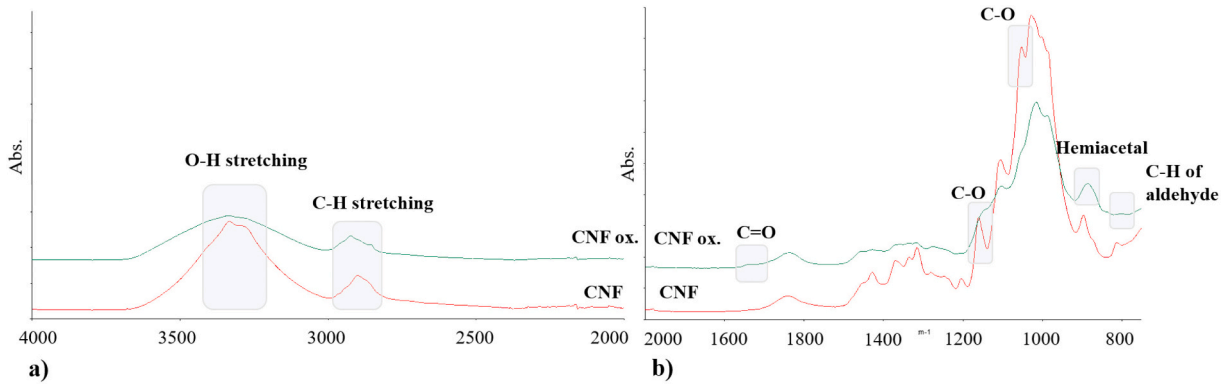

Fig. 2. FTIR spectra for unoxidized and oxidized CNF films. Wavenumber range: a) 4000–2000 cm^{-1}, b) 2000–700 cm^{-1}.

required using $NaBH_4$ at room temperature for 1 h to strengthen covalent bonds between amine and aldehyde groups. Laccase activity was assessed by using a mixture of 500 μL of water and ABTS (the substrate) at the optimum temperature for the enzyme (50 °C) to deposit the films and measuring the absorbance at 436 nm after 0, 30 and 60 s to calculate the amount of laccase immobilized onto each film.

2.6. Storage stability and reusability of immobilized laccase

The stability of the films containing immobilized laccase was assessed by measuring the enzyme activity after storing at 4 °C for 1, 5, 10, 15, 20 and 40 days. On the other hand, their reusability was assessed by measuring laccase activity over 12 consecutive cycles in order to quantify its losses. The films were thoroughly washed with distilled water between cycles.

2.7. Removal of Methylene Blue

The fact that laccase retained its activity upon immobilization was confirmed by assessing its efficiency in oxidizing the dye Methylene Blue (MB). For this purpose, a methacrylate cuvette was loaded with 2 mL of MB (10 ppm) to assess decomposition of the dye upon contact with the CNF film by measuring the UV–Vis absorbance at 665 nm of the MB solution at intervals from 1 to 90 min. The extent of MB removal was calculated as follows:

$$\text{MB removal } (\%) = [(A_0 - A_t)/A_0] \times 100 \quad (6)$$

where A_0 is the dye absorbance at time zero and A_t that after time t.

3. Results and discussion

3.1. Influence on the production of functional groups

As confirmed by using Pommerening's method, oxidation with periodate produced aldehyde groups (CHO) in cellulose. As can be seen from Fig. 1a, the content in CHO groups of the films increased with treatment time, albeit less markedly after 3 h of reaction. Some authors have reported aldehyde contents of CNF similar to those found here (viz., 0.45–1.43 μmol mg^{-1} after 48 h at 40 °C) [6], but others obtained higher contents (e.g., 8.78 mmol g^{-1} CNC after 2 h at 60 °C [45]; 3.8 mmol g^{-1} CNF after 72 h at 25 °C [46], 3.6 mmol g^{-1} carboxymethylated CNF after 24 h at 25 °C [47]; 1.5–6.5 mmol g^{-1} softwood cellulose pulp after 10–96 h [48] or 4.21 mmol g^{-1} cellophane after 6 h [45]). The latter values, however, were obtained by using cellulose suspensions rather than films as here —and films are known to be less prone to forming aldehyde groups.

The conversion of hydroxyl groups in cellulose to aldehyde groups by oxidation with periodate can also be confirmed by measuring antioxidant capacity. Thus, an antioxidant is capable of reducing free radicals.

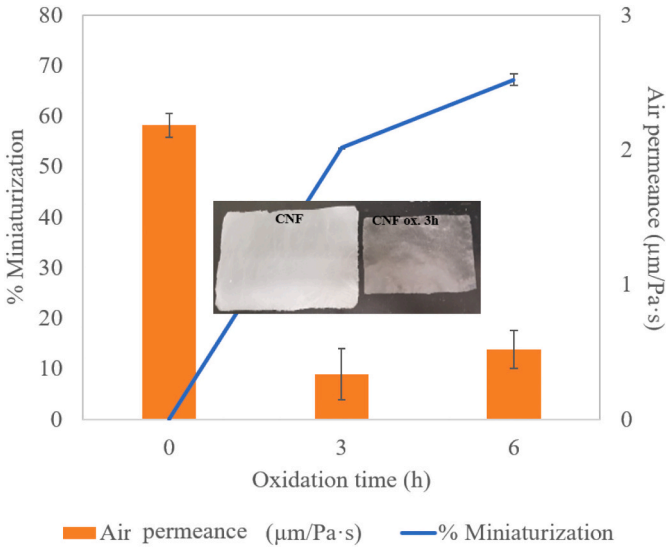

Fig. 3. % Percent miniaturization and air permeance of CNF films oxidized with periodate for 0, 3 and 6 h.

Because hydroxyl groups can act as reductants and CHO groups as oxidants [38], oxidized films should exhibit a decreased antioxidant capacity. As can be seen in Fig. 1b, the antioxidant capacity of the films decreased with time and, consistent with the previous comment, their content in CHO groups increased in parallel. Therefore, antioxidant capacity can provide an indirect measure for CHO content in periodate-oxidized films —a property that should decrease as more cellulose is oxidized.

Oxidation of the films and the presence of aldehyde groups were also confirmed by FTIR spectroscopy. IR analysis was performed on both sides of the film, showing the same spectra and behaviours suggesting that oxidation took place throughout the depth of the film. Fig. 2a shows the FTIR spectra over the wavenumber range 4000–2000 cm^{-1} for oxidized and unoxidized nanocellulose. As can be seen, the peak at 3400 cm^{-1}, corresponding to O—H bonds, decreased in relation to that at 2900 cm^{-1}, due to C—H bonds, and broadened upon oxidation [49]. The decrease is consistent with partial oxidation of hydroxyl groups to aldehyde groups. Also, the peak at 3400 cm^{-1} was slightly blue-shifted by effect of the reduction of hydrogen bonds. Fig. 2b shows the FTIR spectra obtained over the wavenumber range 2000–700 cm^{-1}. The presence of a peak at 1740 cm^{-1} due to C═O bonds confirms that the films were oxidized [50]. The peak, due to free aldehydes, was weak as the likely result of most aldehyde groups being masked as hemiacetal, hydrate or hemialdal forms [51]. The peaks at 880 and 790 cm^{-1}, due to hemiacetals and aldehydes, respectively, were higher in oxidized CNF

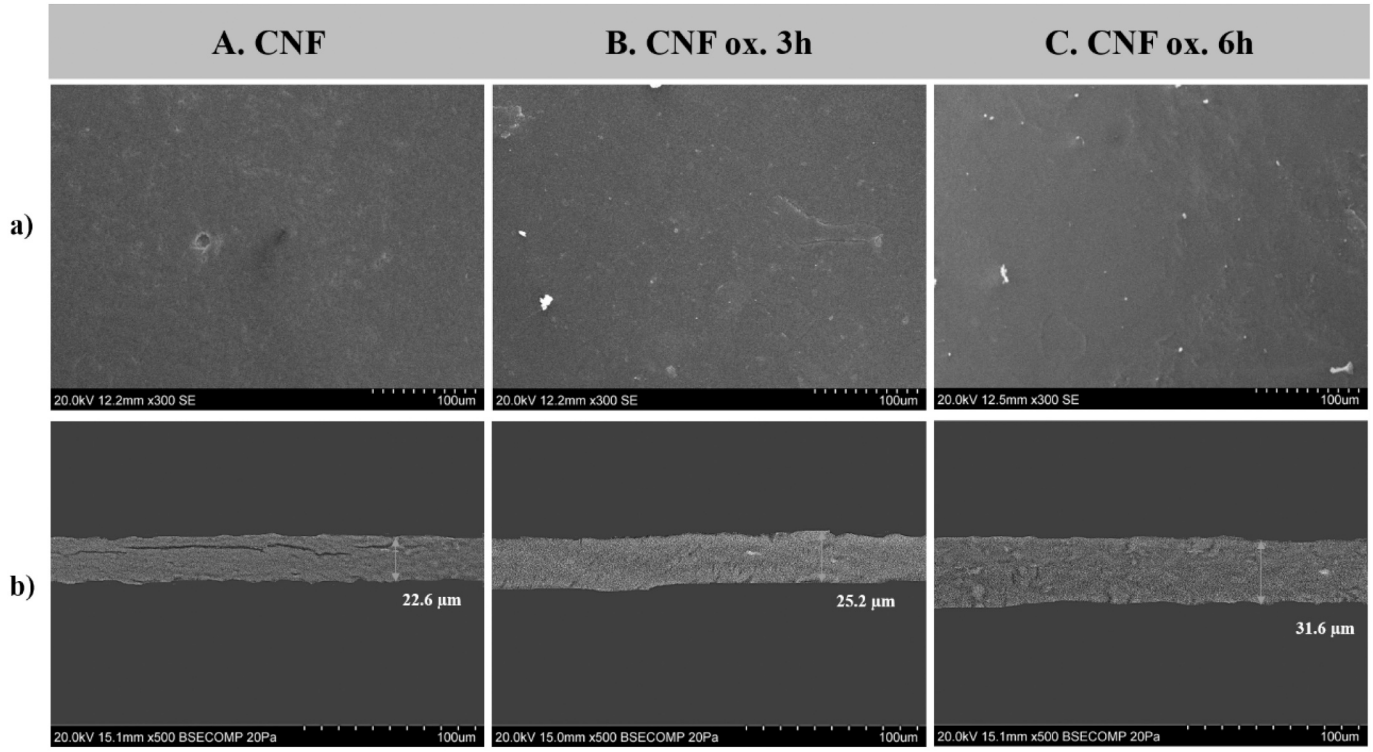

Fig. 4. SEM images of the films CNF, CNF ox. 3 h and CNF ox. 6 h.

because its hemiacetal form was oxidized [52], whereas those at 1160 and 1050 cm^{-1}, due to C–O bonds in cellulose, exhibited the opposite trend [53]. Therefore, the FTIR spectra confirmed that nanocellulose was functionalized with dialdehyde groups.

3.2. Influence on film morphology

One morphological effect of the oxidation treatment on the films was that their surface area decreased with the reaction time. As can be seen from Fig. 3, the decrease amounted to 53.7 % after 3 h and 67 % after 6 h. Film thickness increased with increasing surface area: from 22.6 µm in unoxidized CNF to 25.2 µm after 3 h of oxidation and 32.9 µm after 6 h. Indeed, Strong et al. [54] successfully used oxidation with periodate as a paper miniaturization method that performed optimally with a periodate concentration of 0.6 M and a reaction time of 48 h. They found a direct relationship between the decrease in surface area and oxidation time in various types of cellulose-based membranes. Interestingly, however, membranes made from cellulose derivatives exhibited no decrease in surface area. The effects of periodate were influenced by the temperature, pH and electrolyte concentration [55] —we conducted no similar tests, however. The shrinking effect may have resulted from the formation of intramolecular hemiacetal bonds between aldehyde groups and primary hydroxyl groups in 2,3-dialdehyde cellulose. This intramolecular conversion is impossible in a chair conformation, so it must lead to non-linear, folded, more compact (miniaturized) conformations [56]. In fact, our FTIR spectra confirmed the presence of hemiacetal groups in the oxidized films (see Fig. 2).

As shown by the air permeance results, shrinkage of the films increased their compactness. Unoxidized film had a permeance of 2.18 ± 0.09 µm Pa^{-1} s^{-1} (Fig. 3) that decreased as the oxidation reaction

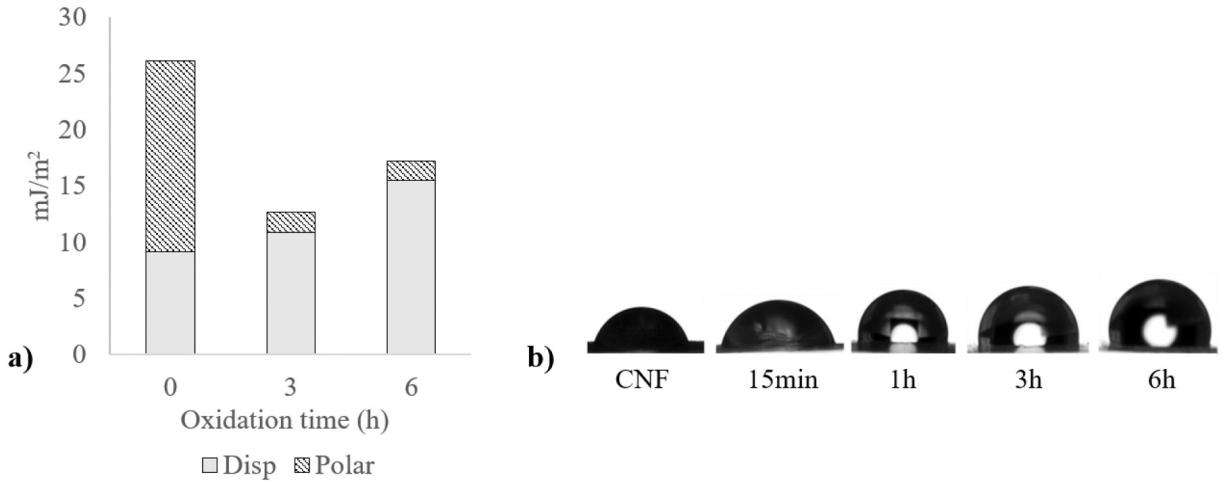

Fig. 5. a) Surface free energy (SFE) and b) water contact angle (WCA) of CNF films oxidized with periodate for 0, 3 and 6 h.

Table 1
WDT, WCA and WVTR at 50 % RH of CNF films oxidized for 0, 3 and 6 h.

Oxidation time (h)	WDT (min)	WCA (°)	WVTR (g m^{-2} day^{-1})
0	46.5 ± 1.0	51.7 ± 6.0	3.31 ± 0.27
3	138.0 ± 3.2	97.4 ± 2.7	2.09 ± 0.32
6	141.0 ± 5.1	102.0 ± 4.5	0.79 ± 0.26

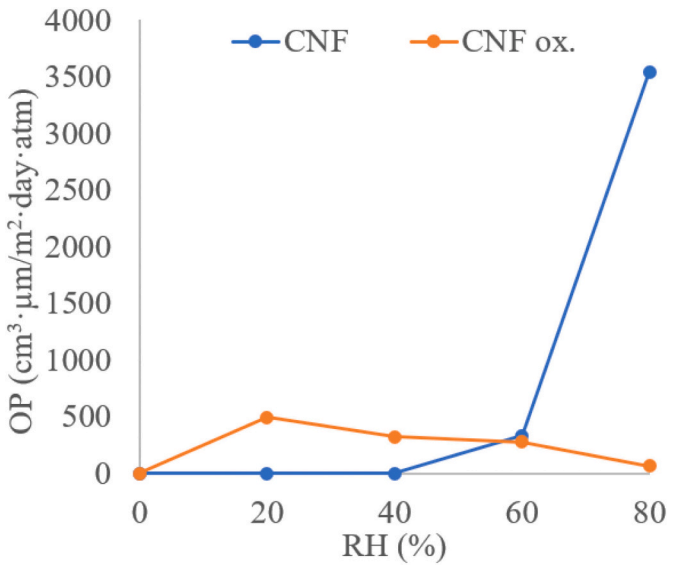

Fig. 6. Oxygen permeability (OP) at a variable relative humidity (RH) of an unoxidized CNF film, and one oxidized with periodate for 3 h.

developed (see Table S1 in Supplementary material). Such a high resistance is very interesting and might enable the use of oxidized films in packaging applications. In fact, previous attempts at obtaining CNC [13] or bacterial cellulose (BC) [57] with favourable barrier properties provided lower air resistance levels than periodate-oxidized CNF.

Scanning electron micrographs revealed very smooth surfaces in both unoxidized CNF (Fig. 4A.a) and in films oxidized for 3 h (Fig. 4B.a) or, especially, 6 h (Fig. 4C.a). In fact, cross-sectional views (Figs. 4A.b, B.b and C.c) confirmed a more compact appearance in the periodate-oxidized films as a result of the formation of hemiacetal and hemialdal bonds during the reaction. Also, the films became not only more compact but also, as noted earlier, thicker, as the reaction developed.

3.3. Surface free energy and permeance

The surface free energy of the films was determined in order to predict their interactions with various liquids. As can be seen from Fig. 5a, SFE for the oxidized films was lower than previously reported values for CNC-based films [13,58] —even though the dispersive contribution of the oxidized films was greater, the polar contribution was much smaller. The decreased polarity of the oxidized films was confirmed by depositing a drop of a polar liquid (water) onto their surface and measuring the resulting water drop test (WDT) and water contact angle (WCA) values (Fig. 5b, Table 1). The contact angle of the films oxidized for 6 h, 102.5°, was much higher than that of the control film (51.62°) and substantially higher than previously reported values for periodate-oxidized nanocellulose [51]. Also, the oxidized films became hydrophobic (WCA > 90°) after 1 h of reaction, probably as a result of miniaturization reducing pore volume [54] or hydroxyl groups being converted into aldehyde groups [51,54]. Also, based on the WDT results (Table 1), the oxidized films possessed a much higher water resistance than the control film, thus confirming the increased compactness of the former. WDT values virtually levelled off after 1 h. The absence of interactions between water and the oxidized films, and their decreased absorption of moisture, can be ascribed to the formation of aldehyde groups from free hydroxyl groups —the latter can interact with water— and also to the increased compactness additionally suggested by the air permeance values.

Table 1 also shows the water vapour permeability at 50 % RH of oxidized and unoxidized CNF films. WVTR decreased with time. As suggested by the miniaturization results and SEM images, the oxidation treatment increased film density and compactness, thereby hindering penetration of water vapour molecules. Also, the increased contact angles and decreased WVTR values obtained are consistent with an increased water resistance in the periodate-oxidized CNF films,

The decreased film polarity inferred from the SFE results also influenced oxygen resistance. Unlike water, oxygen is non-polar. As can be seen from Fig. 6, the films oxidized for 3 h exhibited decreased oxygen resistance at low RH levels, possibly as a result of an increased dispersive component and decreased polar component allowing easy penetration of a non-polar gas such as oxygen.

As can be seen from Fig. 6, oxygen permeability (OP) in the unoxidized film increased markedly at RH > 60 % and reached 50,000 cm^3 µm m^{-2} day^{-1} atm^{-1} at RH = 90 % (unplotted value). By contrast, OP in the oxidized films remained constant or even decreased with increase in RH. The low oxygen permeability of the films even at high RH levels is a distinctive feature of other biopolymers, where OP tends to increase with increasing relative humidity.

The films oxidized for 3 h exhibited a low oxygen permeability. In fact, their OP values were similar to those of commercially available

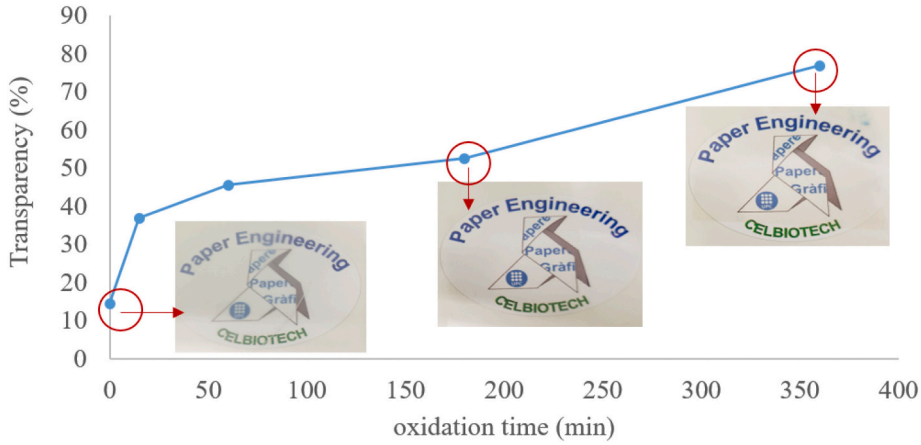

Fig. 7. Percent transparency of an unoxidized CNF film and others oxidized for variable lengths of time.

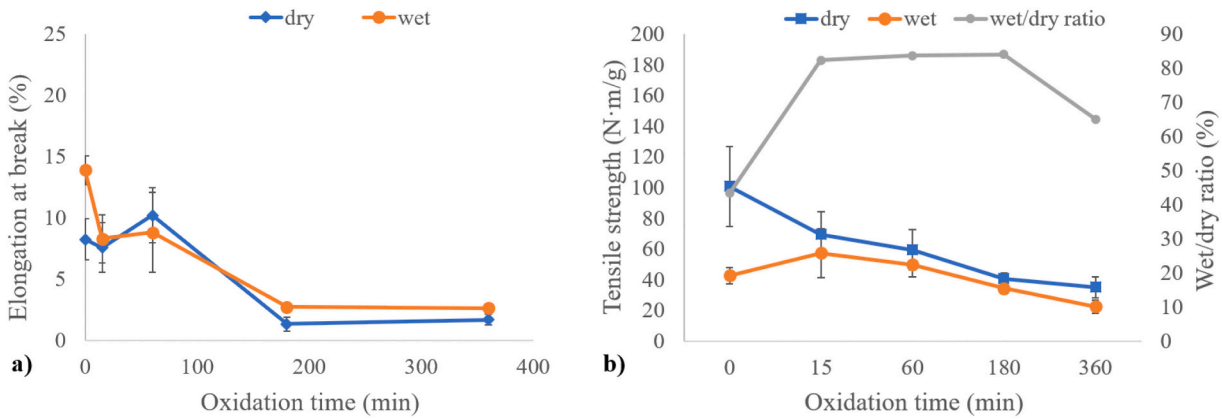

Fig. 8. Mechanical properties of an unoxidized CNF film and others oxidized for variable lengths of time.

materials with favourable oxygen-barrier properties such as poly (ethylene-*co*-vinyl alcohol), high-density polyethylene, poly(ethylene terephthalate), nylon-6, poly(vinylidene chloride) or poly(vinyl alcohol) [59,60]. This makes periodate-oxidized CNF film an attractive choice for packaging food that is very difficult to preserve in non-plastic materials. Other authors have reported similar OP values for periodate-oxidized films at low RH levels [51] but seemingly none obtained at high RH levels.

Oil resistance is one other important property for packaging films. All unoxidized and periodate-oxidized films studied here were oil-resistant. In fact, none showed any signs of oil penetration even after 1800 s. Some authors have found nanocellulose to be oil-resistant. Thus, Fernández-Santos et al. [61] reported oil resistance values similar to ours albeit for CNF–CNC and CNF–MCC films. CNC systems doped with various natural additives also exhibit similar oil resistance values [13]. Although a decrease in the polar component may have increased oil absorption, the much greater compactness and density of the oxidized films prevented oil absorption from increasing upon oxidation with periodate.

3.4. Effects on optical and mechanical properties

Transparency can be a desirable attribute of some products. Improving the typically good transparency of CNF films is difficult, however [15]. Fig. 7 shows the transparency of CNF films oxidized with periodate for variable lengths of time. As can be seen, this property increased with treatment time, from 14 % in the unoxidized film to 77 % after 6 h. The transparency values for the films oxidized for 3 h were similar to those reported for crystalline nanocellulose (56.08 %, [61]), whereas those obtained after oxidation for 6 h were very high and similar to those for other cellulose derivatives such as microcrystalline cellulose (MCC, 77.85 % [61]). An increased transparency was also observed by other authors who obtained 2,3-dialdehyde cellulose (DAC) by oxidizing MCC with sodium periodate at 48 °C for 19 h [51].

The CNF films were also examined for mechanical properties under both dry and wet conditions. The extent of hydration of aldehyde groups strongly influences the formation of hemiacetal and hemialdal networks, and hence mechanical properties. As can be seen from Fig. 8a, elongation decreased as the oxidation treatment progressed in both dry

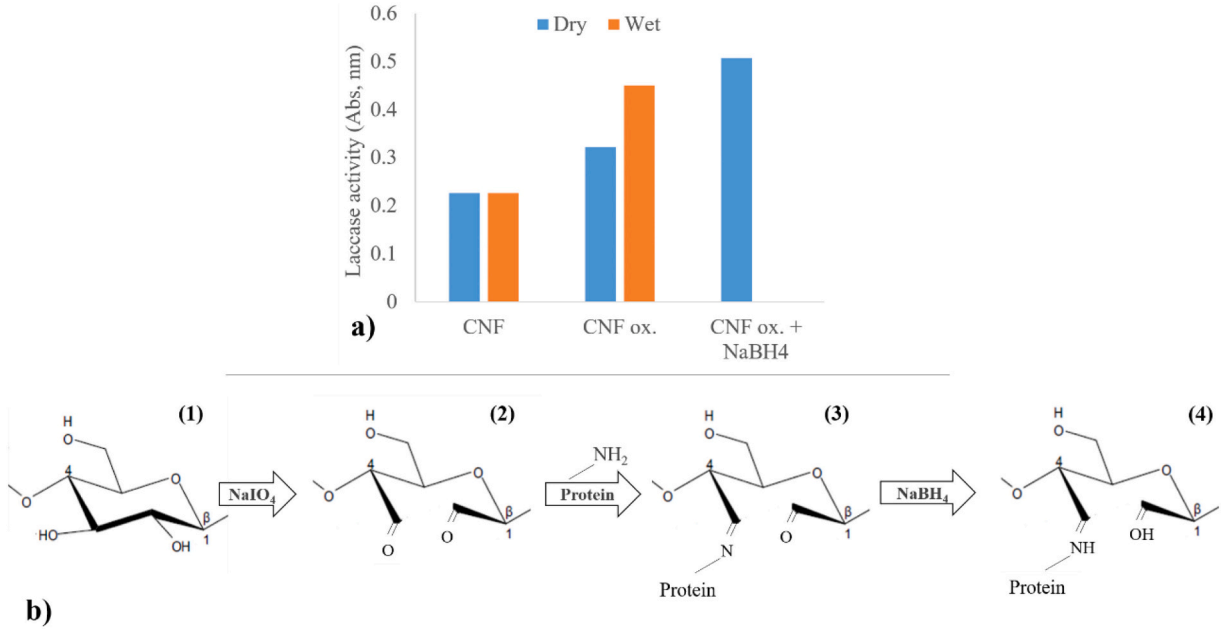

Fig. 9. a) Dry and wet activity of laccase immobilized onto an unoxidized CNF film and an oxidized one in the presence and absence of $NaBH_4$. b) Schematic representation of the binding process of a protein to oxidized cellulose: (1) unoxidized cellulose molecule; (2) oxidized cellulose molecule with aldehyde groups already present; (3) binding of the amino group of the protein to the aldehyde of the cellulose forming a reversible Schiff base; (4) reduction of the remaining aldehyde and the non-reversible Schiff base.

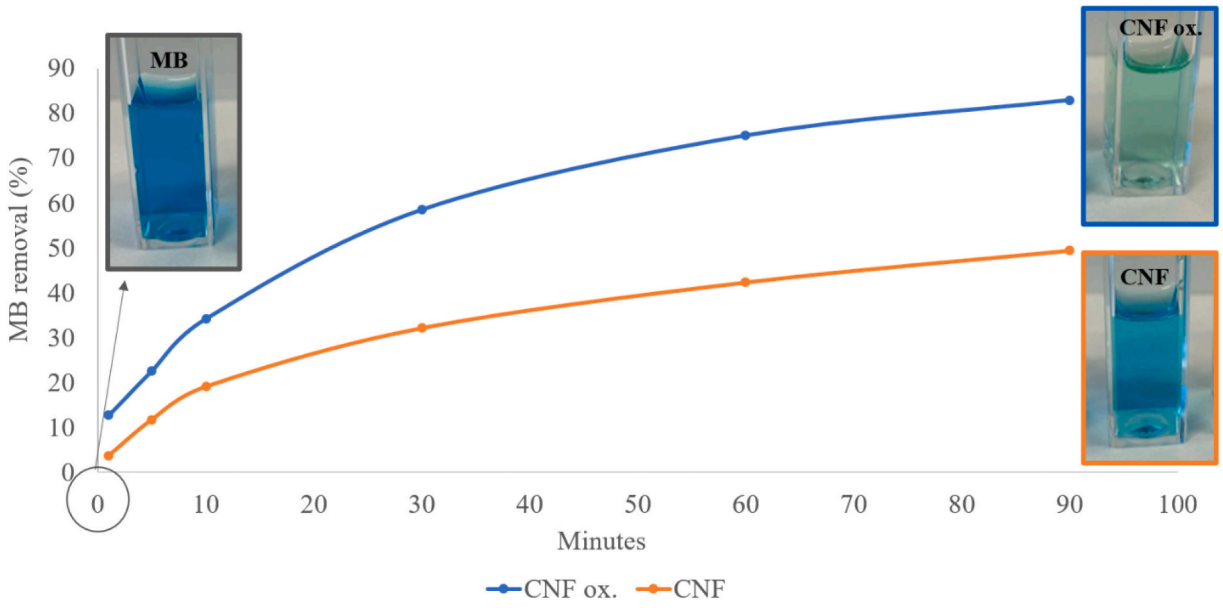

Fig. 10. Variation of the extent of Methylene Blue (MB) removal by an oxidized CNF film (CNF ox.) containing immobilized laccase, and one containing no enzyme (CNF), with time and appearance of the MB solution before and after contact with the laccase-containing film.

and wet tests. This behaviour can be explained by the formation of hemiacetals between aldehyde (generated during periodate oxidation) and alcohol groups, as has already been described by other authors. They state that the presence of aldehyde groups formed during TEMPO oxidation of cotton linters [62] and hardwood bleached kraft pulp [63] produced a decrease in elongation due to the formation of hemiacetals. Wet elongation exceeded dry elongation by effect of water slightly weakening bonds and allowing nanocellulose structures more freedom as a result.

As can be seen from Fig. 8b, dry and wet tensile strength decreased with time. However, the control film behaved differently from the treated films. Thus, the former exhibited a considerably high dry strength that was much lower than its wet strength. On the other hand, the oxidized films exhibited less marked differences between their dry and wet values. The previous differences reflected in the wet/dry ratio, which was used to relate tensile strength under wet and dry conditions. As can be seen from Fig. 8b, such a ratio increased with treatment time. Thus, the ratio of the films treated for 3 h was 84.1 %, so the films only lost 15.9 % of their tensile strength upon wetting. On the other hand, the ratio for the unoxidized film was 43.3 % and it lost 56.6 % of its strength by effect of moisture. Therefore, moisture considerably reduced the tensile strength of the unoxidized CNF film but not that of the oxidized films even though the latter were weaker than was the former under dry conditions. This was a result of the number of hemiacetal and hemialdal groups increasing with oxidation time and covalent bonds replacing the typical hydrogen bonds, thereby lessening the impact of water on the films [22]. This assumption is consistent with the fact that the dry tensile strength decreased with time in the periodate treatment. In fact, oxidation of hydroxyl groups to aldehyde groups partially hindered the formation of hydrogen bonds, which are responsible for dry tensile strength [64]. By contrast, the process caused the formation of hemiacetal and hemialdal groups, which might be responsible for the virtual absence of tensile strength losses in the wet films [22]. The high wet strength of the oxidized films is very interesting as it can allow their use unaltered in water.

3.5. Production of active packaging

In further tests, we examined whether the presence of aldehyde groups would allow an enzyme such as laccase to be immobilized in order to obtain active packaging preventing food deterioration. The enzyme was immobilized onto two different supports, namely: a periodate-treated film that was dried after oxidation (CNF ox. Dry) and a similarly treated film that was not dried after treatment (CNF ox. Wet). The enzyme, which was immobilized by following the same procedure in both cases, was assumed to be anchored by covalent bonding, which is usually highly efficient [65].

As can be seen from Fig. 9a, the amount of laccase immobilized onto CNF ox. Dry was increased by the presence of $NaBH_4$, which promoted stronger bonding between the enzyme and aldehyde groups through the formation of secondary amine groups (−NH) [66,67]. This allowed aldehyde−enzyme bonds to retain their strength after thorough washing with water. In the absence of $NaBH_4$, bonds were weaker and the amount of enzyme immobilized was smaller as a result. Such an amount was smaller in the oxidized films than it was in the unoxidized film whether $NaBH_4$ was present or absent from the reaction medium.

As can be seen from the results for the film CNF ox. Dry, aldehyde−enzyme bonds were seemingly more stable and led to more efficient immobilization of the enzyme even after the film was washed. On the other hand, the film CNF ox. Wet was destroyed by $NaBH_4$ so no laccase immobilizations measurements could be made on it. In Fig. 9b, a schematic representation of the binding process with a protein and the oxidized cellulose can be seen. It is also shown how $NaBH_4$ leads to the reduction of the remaining aldehyde and favours the formation of the non-reversible Schiff base.

The functionality of laccase immobilized on the oxidized films was assessed as the enzyme's ability to degrade the dye Methylene Blue (MB). As can be seen from Fig. 10, the film containing immobilized laccase was more efficient in decolorizing the dye. Thus, MB was removed by 47 % from the control film (CNF), and by 80 % from the laccase-containing film, after 90 min and the proportion increased with time in the latter case (Fig. 10). As previously found by other authors [68–72], laccase was highly efficient in degrading MB. Based on the results, the enzyme immobilized onto a periodate-oxidized CNF film performed quite well as a catalyst and can therefore be a good choice for use in active packaging.

3.6. Storage stability and reusability of immobilized laccase

The industrial use of laccase is limited by its tendency to loss enzymatic activity under extreme conditions [31]. Also, the enzyme is poorly

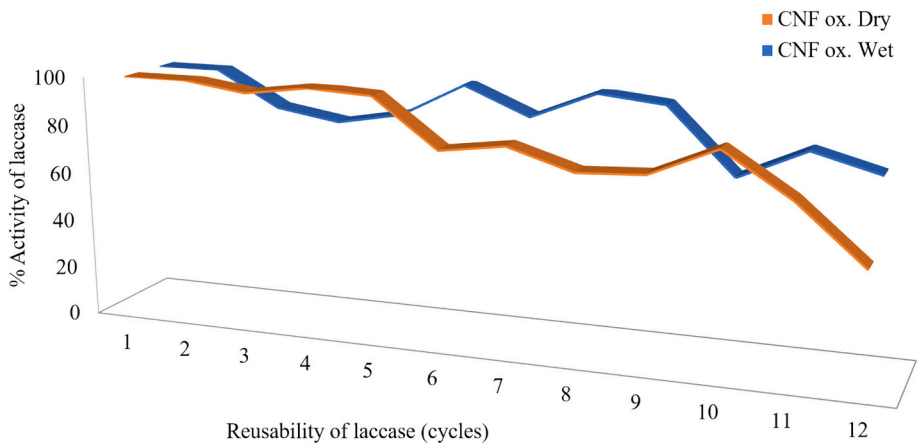

Fig. 11. Reusability of laccase immobilized on the oxidized films CNF ox. Dry and CNF ox. Wet.

reusable and rather unstable. In fact, immobilization alters the structure of enzymes and hence their stability.

Retaining their properties with time is a great asset for functionalized CNF films, especially if they are not intended for immediate use. We assessed the stability of the films CNF ox. Dry and CNF ox. Wet containing immobilized laccase after storage for 30 days by measuring their activity at 2-day intervals. The results were quite good. In fact, immobilized laccase retained its activity after 30 days of storage at 4 °C under both dry and wet conditions (results not shown). Chatterjee et al. [28] obtained similarly good results with laccase also stored at 4 °C.

The ability to reuse the immobilized enzyme reduces the overall cost of enzyme-catalysed industrial processes and is crucial with a view to obtaining reusable packaging and mitigating current environmental pollution problems. Laccase reusability was assessed here over 12 consecutive cycles. The activity of the original laccase was taken to be 100 % and, as can be seen from Fig. 11, the film CNF ox. Dry retained >75 % of the activity until cycle 11, and so did CNF ox. Wet until cycle 12. The 25 % decrease observed may have resulted from denaturation of the enzyme [73]. The activity of laccase immobilized on CNF ox. Dry remained stable until cycle 5 and decreased afterwards, albeit only to 79 %. The activity retention results obtained with both films are better than those reported by other authors. Thus, Xing et al. [33] reported 67 % for immobilized laccase after 6 cycles; Chen Lin [74] 69 % for laccase immobilized on cellulose from bacterial membranes after 7; and Yinghui et al. [75] 64 % for laccase on poly(vinyl alcohol).

As shown by previous studies, laccase is an effective alternative to the conventional two-enzyme system (glucose oxidase–catalase) typically used in food packaging [76], which poses some problems arising from the presence of hydrogen peroxide. On the other hand, laccase is able to reduce molecular oxygen to water without the need for hydrogen peroxide. Also, as noted earlier, it is compatible with a broad range of reductive substrates. Other authors have examined the performance of laccase immobilized by trapping onto latex under variable temperature and time conditions [28]. Bioprocess technology has helped reduce enzyme production costs and make enzymes viable choices for industrial uses such as food packaging [28].

4. Conclusions

In this work, cellulose nanofibril (CNF) films were oxidized with periodate for variable lengths of time. The number of aldehyde groups in the films increased with treatment time but levelled off after 3 h. The oxidized films exhibited a decreased antioxidant capacity by effect of the presence of aldehyde groups. As confirmed by FTIR spectra, the treatment also caused the formation of hemiacetal and hemialdal groups in the films that led to their shrinking by up to 67 %. Film compaction was confirmed by SEM images, which revealed an increase in thickness from 22.6 μm in the unoxidized film to 31.6 μm in that oxidized for 6 h (CNF ox. 6 h). Compaction decreased oxygen permeability in the films and increased fat resistance as a result. Also, the oxidized films lost only 16 % of their tensile strength upon immersion in water, whereas the unoxidized film lost as much as 57 %.

Oxidation of hydroxyl groups to aldehyde groups additionally decreased polarity in the films, thereby considerably increasing their hydrophobicity and improving their water vapour barrier properties. Also, the films exhibited excellent oxygen barrier properties (viz., 68.4 cm^3 μm m^{-2} day^{-1} atm^{-1} at 80 % RH and impenetrability at 90 % RH).

Finally, dialdehyde films were used to immobilize laccase for use as active packaging. The films containing immobilized laccase retained their whole activity after storage at 4 °C for 1 month, whereas those reused over 11 or 12 cycles lost <25 % and were highly efficient in degrading the dye Methylene Blue.

Supplementary data to this article can be found online at https://doi.org/10.1016/j.ijbiomac.2024.131553.

CRediT authorship contribution statement

Julia Fernández-Santos: Writing – original draft, Investigation. **Cristina Valls:** Writing – review & editing, Supervision, Conceptualization. **Oriol Cusola:** Writing – review & editing, Conceptualization. **M. Blanca Roncero:** Writing – review & editing, Supervision, Funding acquisition, Conceptualization.

Declaration of competing interest

The authors declare that they have no known competing financial interests or personal relationships that could have appeared to influence the work reported in this paper.

Data availability

All the data are included in the figures and table of the paper

Acknowledgments

This publication is part of the PID2020-114070RB-I00 (CELLECOPROD) project, funded by MCIN/AEI/10.13039/501100011033. The authors would also like to thank the consolidated research group AGAUR 2021 SGR 00852. The first author, J. Fernández-Santos, acknowledges the Universitat Politècnica de Catalunya and the Generalitat de Catalunya for the financial support of her predoctoral grant FI.

References

[1] D.S. Lakshmi, N. Trivedi, C.R.K. Reddy, Synthesis and characterization of seaweed cellulose derived carboxymethyl cellulose, Carbohydr. Polym. 157 (2017) 1604–1610. https://linkinghub.elsevier.com/retrieve/pii/S0144861716313078.

[2] E. Quintana, M. Ago, C. Valls, M.B. Roncero, O.J. Rojas, Alternative chemo-enzymatic treatment for homogeneous and heterogeneous acetylation of wood fibers, Cellulose 25 (9) (2018) 5323–5336, https://doi.org/10.1007/s10570-018-1947-4.

[3] J. Rojas, Functionalization and crosslinking of microcrystalline cellulose in aqueous media: a safe and economic approach, Int. J. Pharm. Sci. Rev. Res. 8 (1) (2011) 28–36.

[4] F. Beltramino, M.B. Roncero, T. Vidal, A.L. Torres, C. Valls, Increasing yield of nanocrystalline cellulose preparation process by a cellulase pretreatment, Bioresour. Technol. 192 (2015) 574–581, https://doi.org/10.1016/j.biortech.2015.06.007.

[5] O. Nechyporchuk, M.N. Belgacem, J. Bras, Production of cellulose nanofibrils: a review of recent advances, Ind. Crop. Prod. 93 (2016) 2–25, https://doi.org/10.1016/j.indcrop.2016.02.016.

[6] A. Errokh, A. Magnin, J.L. Putaux, S. Boufi, Morphology of the nanocellulose produced by periodate oxidation and reductive treatment of cellulose fibers, Cellulose 25 (7) (2018) 3899–3911.

[7] E. Csiszár, S. Nagy, A comparative study on cellulose nanocrystals extracted from bleached cotton and flax and used for casting films with glycerol and sorbitol plasticisers, Carbohydr. Polym. 174 (2017) 740–749, https://doi.org/10.1016/j.carbpol.2017.06.103.

[8] F. Beltramino, M. Blanca Roncero, T. Vidal, C. Valls, A novel enzymatic approach to nanocrystalline cellulose preparation, Carbohydr. Polym. 189 (February) (2018) 39–47.

[9] N. Grishkewich, N. Mohammed, J. Tang, K.C. Tam, Recent advances in the application of cellulose nanocrystals, Curr. Opin. Colloid Interface Sci. 29 (2017) 32–45, https://doi.org/10.1016/j.cocis.2017.01.005.

[10] J. Tang, J. Sisler, N. Grishkewich, K.C. Tam, Functionalization of cellulose nanocrystals for advanced applications, J. Colloid Interface Sci. 494 (2017) 397–409, https://doi.org/10.1016/j.jcis.2017.01.077.

[11] H.-J. Kim, S. Roy, J.-W. Rhim, Effects of various types of cellulose nanofibers on the physical properties of the CNF-based films, J. Environ. Chem. Eng. 9 (5) (2021) 106043, https://doi.org/10.1016/j.jece.2021.106043.

[12] C. Valls, F.I.J. Pastor, M.B. Roncero, T. Vidal, P. Diaz, J. Martínez, et al., Assessing the enzymatic effects of cellulases and LPMO in improving mechanical fibrillation of cotton linters, Biotechnol. Biofuels 12 (1) (2019) 161, https://doi.org/10.1186/s13068-019-1502-z.

[13] J. Fernández-Santos, C. Valls, O. Cusola, M.B. Roncero, Improving filmogenic and barrier properties of nanocellulose films by addition of biodegradable plasticizers, ACS Sustain. Chem. Eng. 9 (29) (2021) 9647–9660, https://doi.org/10.1021/acssuschemeng.0c09109.

[14] P. Tyagi, L.A. Lucia, M.A. Hubbe, L. Pal, Nanocellulose-based multilayer barrier coatings for gas, oil, and grease resistance, Carbohydr. Polym. 206 (October 2018) (2019) 281–288, https://doi.org/10.1016/j.carbpol.2018.10.114.

[15] L. Zhang, J. Zhao, Y. Zhang, F. Li, X. Jiao, Q. Li, The effects of cellulose nanocrystal and cellulose nanofiber on the properties of pumpkin starch-based composite films, Int. J. Biol. Macromol. 192 (17) (2021) 444–451, https://doi.org/10.1016/j.ijbiomac.2021.09.187.

[16] E. Quintana, M.B. Roncero, T. Vidal, C. Valls, Cellulose oxidation by Laccase-TEMPO treatments, Carbohydr. Polym. 157 (2017) 1488–1495, https://doi.org/10.1016/j.carbpol.2016.11.033.

[17] C. Valls, O. Cusola, M.B. Roncero, Evaluating the potential of ozone in creating functional groups on cellulose, Cellulose 29 (12) (2022) 6595–6610, https://doi.org/10.1007/s10570-022-04694-4.

[18] S. Coseri, G. Biliuta, B.C. Simionescu, K. Stana-Kleinschek, V. Ribitsch, V. Harabagiu, Oxidized cellulose - survey of the most recent achievements, Carbohydr. Polym. 93 (1) (2013) 207–215, https://doi.org/10.1016/j.carbpol.2012.03.086.

[19] M. Hietala, A. Ämmälä, J. Silvennoinen, H. Liimatainen, Fluting medium strengthened by periodate–chlorite oxidized nanofibrillated celluloses, Cellulose 23 (1) (2016) 427–437.

[20] K. Pommerening, H. Rein, D. Bertram, R. Müller, Estimation of dialdehyde groups in 2,3-dialdehyde bead-cellulose, Carbohydr. Res. 233 (C) (1992) 219–223.

[21] H. Galbraith, T.B. Miller, A.M. Paton, J.K. Thompson, Antibacterial activity of long chain fatty acids and the reversal with calcium, magnesium, ergocalciferol and cholesterol, J. Appl. Bacteriol. 34 (4) (1971) 803–813.

[22] T. Nypelö, H. Amer, J. Konnerth, A. Potthast, T. Rosenau, Self-standing nanocellulose janus-type films with aldehyde and carboxyl functionalities, Biomacromolecules 19 (3) (2018) 973–979.

[23] S.M.A.S. Keshk, S. Bondock, A.A. El-Zahhar, M.A. Haija, Synthesis and characterization of novel Schiff's bases derived from dialdehyde cellulose-6-phosphate, Cellulose 26 (6) (2019) 3703–3712, https://doi.org/10.1007/s10570-019-02360-w.

[24] J.R. Westlake, M.W. Tran, Y. Jiang, X. Zhang, A.D. Burrows, M. Xie, Biodegradable active packaging with controlled release: principles, progress, and prospects, ACS Food Sci. Technol. 2 (8) (2022) 1166–1183.

[25] S. Yildirim, B. Röcker, M.K. Pettersen, J. Nilsen-Nygaard, Z. Ayhan, R. Rutkaite, et al., Biodegradable active packaging with controlled release: principles, progress, and prospects, ACS Food Sci. Technol. 17 (1) (2018) 165–199.

[26] Huis In''t Veld JHJHI, Microbial and biochemical spoilage of foods: an overview, Int. J. Food Microbiol. 33 (1) (1996) 1–18.

[27] M. Ozdemir, J.D. Floros, Active food packaging technologies, Crit. Rev. Food Sci. Nutr. 44 (3) (2004) 185–193.

[28] R. Chatterjee, K. Johansson, L. Järnström, L.J. Jönsson, Evaluation of the potential of fungal and plant laccases for active-packaging applications, J. Agric. Food Chem. 59 (10) (2011) 5390–5395.

[29] D.M. Mate, M. Alcalde, Laccase: a multi-purpose biocatalyst at the forefront of biotechnology, Microb. Biotechnol. 10 (6) (2017) 1457–1467.

[30] D. Ibarra, J. Romero, M.J. Martínez, A.T. Martínez, S. Camarero, Exploring the enzymatic parameters for optimal delignification of eucalypt pulp by laccase-mediator, Enzym. Microb. Technol. 39 (6) (2006) 1319–1327.

[31] O. Cusola, C. Valls, T. Vidal, M.B. Roncero, Application of surface enzyme treatments using laccase and a hydrophobic compound to paper-based media, Bioresour. Technol. 131 (2013) 521–526, https://doi.org/10.1016/j.biortech.2012.12.186.

[32] P.J. Strong, H. Claus, Laccase: a review of its past and its future in bioremediation, Crit. Rev. Environ. Sci. Technol. 41 (4) (2011) 373–434.

[33] X. Xing, Y. Han, Q. Jiang, Y. Sun, X. Wang, G. Qu, et al., Immobilization of laccases onto cellulose nanocrystals derived from waste newspaper: relationship between immobilized laccase activity and dialdehyde content, Cellulose 28 (8) (2021) 4793–4805, https://doi.org/10.1007/s10570-021-03867-x.

[34] T. Nikolic, M. Kostic, J. Praskalo, B. Pejic, Z. Petronijevic, P. Skundric, Sodium periodate oxidized cotton yarn as carrier for immobilization of trypsin, Carbohydr. Polym. 82 (3) (2010) 976–981, https://doi.org/10.1016/j.carbpol.2010.06.028.

[35] M. Fernández-Fernández, M.Á. Sanromán, D. Moldes, Recent developments and applications of immobilized laccase, Biotechnol. Adv. 31 (8) (2013) 1808–1825.

[36] N. Jaiswal, V.P. Pandey, U.N. Dwivedi, Immobilization of papaya laccase in chitosan led to improved multipronged stability and dye discoloration, Int. J. Biol. Macromol. 86 (2016) 288–295.

[37] R. Wu, B.H. He, G.L. Zhao, L.Y. Qian, X.F. Li, Immobilization of pectinase on oxidized pulp fiber and its application in whitewater treatment, Carbohydr. Polym. 97 (2) (2013) 523–529, https://doi.org/10.1016/j.carbpol.2013.05.019.

[38] N. Drogat, R. Granet, V. Sol, A. Memmi, Antimicrobial Silver Nanoparticles Generated on Cellulose Nanocrystals, 2011, pp. 1557–1562.

[39] S. Iwamoto, A.N. Nakagaito, H. Yano, Nano-fibrillation of pulp fibers for the processing of transparent nanocomposites, Appl. Phys. A Mater. Sci. Process. 89 (2) (2007) 461–466.

[40] T.M.P. Ngo, T.M.Q. Dang, T.X. Tran, P. Rachtanapun, Effects of zinc oxide nanoparticles on the properties of pectin/alginate edible films, Int. J. Polym. Sci. 2018 (2018) 1–9. https://www.hindawi.com/journals/ijps/2018/5645797/.

[41] G.S. Marques, G.R. de Carvalho, N.P. Marinho, G.I.B. de Muniz, L.M. de Matos Jorge, R.M.M. Jorge, Production and characterization of starch-based films reinforced by ramie nanofibers (Boehmeria nivea), J. Appl. Polym. Sci. 136 (36) (2019) 1–11.

[42] M. Dick, T.M.H. Costa, A. Gomaa, M. Subirade, A.D.O. Rios, S.H. Flôres, Edible film production from chia seed mucilage: effect of glycerol concentration on its physicochemical and mechanical properties, Carbohydr. Polym. 130 (2015) 198–205, https://doi.org/10.1016/j.carbpol.2015.05.040.

[43] J.H. Han, J.D. Floros, Casting antimicrobial packaging films and measuring their physical properties and antimicrobial activity, J. Plast. Film Sheeting 13 (4) (1997) 287–298.

[44] D.K. Owens, R.C. Wendt, Estimation of the surface free energy of polymers, J. Appl. Polym. Sci. 13 (8) (1969) 1741–1747, https://doi.org/10.1002/app.1969.070130815.

[45] C. Gao, S. Wang, B. Liu, S. Yao, Y. Dai, L. Zhou, et al., Sustainable chitosan-dialdehyde cellulose nanocrystal film, Materials (Basel) 14 (19) (2021).

[46] K. Zhang, M. Shen, H. Liu, S. Shang, D. Wang, H. Liimatainen, Facile synthesis of palladium and gold nanoparticles by using dialdehyde nanocellulose as template and reducing agent, Carbohydr. Polym. 186 (16) (2018) 132–139, https://doi.org/10.1016/j.carbpol.2018.01.048.

[47] R. Hollertz, V.L. Durán, P.A. Larsson, L. Wågberg, Chemically modified cellulose micro- and nanofibrils as paper-strength additives, Cellulose 24 (9) (2017) 3883–3899.

[48] H. Yang, M.N. Alam, T.G.M. van de Ven, Highly charged nanocrystalline cellulose and dicarboxylated cellulose from periodate and chlorite oxidized cellulose fibers, Cellulose 20 (4) (2013) 1865–1875.

[49] X. Tian, X. Jiang, Preparing water-soluble 2, 3-dialdehyde cellulose as a bio-origin cross-linker of chitosan, Cellulose 25 (2) (2018) 987–998, https://doi.org/10.1007/s10570-017-1607-0.

[50] L. Münster, J. Vícha, J. Klofáč, M. Masař, P. Kucharczyk, I. Kuřitka, Stability and aging of solubilized dialdehyde cellulose, Cellulose 24 (7) (2017) 2753–2766.

[51] S.F. Plappert, S. Quraishi, N. Pircher, K.S. Mikkonen, S. Veigel, K.M. Klinger, et al., Transparent, flexible, and strong 2,3-dialdehyde cellulose films with high oxygen barrier properties, Biomacromolecules 19 (7) (2018) 2969–2978.

[52] H. Liimatainen, M. Visanko, J.A. Sirviö, O.E.O. Hormi, J. Niinimaki, Enhancement of the nanofibrillation of wood cellulose through sequential periodate-chlorite oxidation, Biomacromolecules 13 (5) (2012) 1592–1597.

[53] U.J. Kim, M. Wada, S. Kuga, Solubilization of dialdehyde cellulose by hot water, Carbohydr. Polym. 56 (1) (2004) 7–10.

[54] E.B. Strong, C.W. Kirschbaum, A.W. Martinez, N.W. Martinez, Paper miniaturization via periodate oxidation of cellulose, Cellulose 25 (6) (2018) 3211–3217, https://doi.org/10.1007/s10570-018-1805-4.

[55] T.P. Nevell, 35—the mechanism of the oxidation of cellulose by periodate, J. Text. Inst. Trans. 48 (12) (1957) T484–T494.

[56] R.D. Guthrie, The "dialdehydes" from the periodate oxidation of carbohydrates, Adv. Carbohydr. Chem. 16 (C) (1962) 105–158.

[57] A. Fillat, J. Martínez, C. Valls, O. Cusola, M.B. Roncero, T. Vidal, et al., Bacterial cellulose for increasing barrier properties of paper products, Cellulose 25 (10) (2018) 6093–6105, https://doi.org/10.1007/s10570-018-1967-0.
[58] X. Sun, C. Mei, A.D. French, S. Lee, Y. Wang, Q. Wu, Surface wetting behavior of nanocellulose-based composite films, Cellulose 25 (9) (2018) 5071–5087, https://doi.org/10.1007/s10570-018-1927-8.
[59] C.N. Wu, T. Saito, S. Fujisawa, H. Fukuzumi, A. Isogai, Ultrastrong and high gas-barrier nanocellulose/clay-layered composites, Biomacromolecules 13 (6) (2012) 1927–1932.
[60] Q. Yang, H. Fukuzumi, T. Saito, A. Isogai, L. Zhang, Transparent cellulose films with high gas barrier properties fabricated from aqueous alkali/urea solutions, Biomacromolecules 12 (7) (2011) 2766–2771.
[61] J. Fernández-Santos, C. Valls, O. Cusola, M.B. Roncero, Composites of cellulose nanocrystals in combination with either cellulose nanofibril or carboxymethylcellulose as functional packaging films, Int. J. Biol. Macromol. 211 (May) (2022) 218–229.
[62] L.M. Hillscher, M.V. Höfler, T. Gutmann, C. Lux, K.U. Clerkin, G. Schwall, et al., Influence of TEMPO-oxidation on pulp fiber chemistry, morphology and mechanical paper sheet properties, Cellulose (2024) 0123456789, https://doi.org/10.1007/s10570-024-05748-5.
[63] Y. Kobayashi, T. Gondo, M. Yamamoto, T. Saito, A. Isogai, Fundamental properties of handsheets containing TEMPO-oxidized pulp in various weight ratios, Nord. Pulp Pap. Res. J. 31 (2) (2016) 248–254.
[64] M. Shimizu, T. Saito, H. Fukuzumi, A. Isogai, Hydrophobic, ductile, and transparent nanocellulose films with quaternary alkylammonium carboxylates on nanofibril surfaces, Biomacromolecules 15 (11) (2014) 4320–4325.
[65] S. Yang, Y. Tang, J. Wang, F. Kong, J. Zhang, Surface treatment of cellulosic paper with starch-based composites reinforced with nanocrystalline cellulose, Ind. Eng. Chem. Res. 53 (36) (2014) 13980–13988.
[66] W. Hong, S.G. Jeong, G. Shim, D.Y. Kim, S.P. Pack, C.S. Lee, Improvement in the reproducibility of a paper-based analytical device (PAD) using stable covalent binding between proteins and cellulose paper, Biotechnol. Bioprocess Eng. 23 (6) (2018) 686–692.
[67] N. Isobe, D.S. Lee, Y.J. Kwon, S. Kimura, S. Kuga, M. Wada, et al., Immobilization of protein on cellulose hydrogel, Cellulose 18 (5) (2011) 1251–1256.
[68] N. Popović, D. Pržulj, M. Mladenović, O. Prodanović, S. Ece, K. Ilić Đurđić, et al., Immobilization of yeast cell walls with surface displayed laccase from Streptomyces cyaneus within dopamine-alginate beads for dye decolorization, Int. J. Biol. Macromol. 181 (2021) 1072–1080.
[69] Zabin K. Bagewadi, Sikandar I. Mulla, H.Z. Ninnekar, Purification and Immobilization of Laccase From Trichoderma harzianum Strain HZN10 and Its Application in Dye Decolorization, 2017, pp. 139–150.
[70] A. Kunamneni, I. Ghazi, S. Camarero, A. Ballesteros, F.J. Plou, M. Alcalde, Decolorization of synthetic dyes by laccase immobilized on epoxy-activated carriers, Process Biochem. 43 (2) (2008) 169–178.
[71] D. Daâssi, S. Rodríguez-Couto, M. Nasri, T. Mechichi, Biodegradation of textile dyes by immobilized laccase from Coriolopsis gallica into Ca-alginate beads, Int. Biodeterior. Biodegrad. 90 (2014) 71–78.
[72] M. Mogharabi, N. Nassiri-Koopaei, M. Bozorgi-Koushalshahi, N. Nafissi-Varcheh, G. Bagherzadeh, M.A. Faramarzi, Immobilization of laccase in alginate-gelatin mixed gel and decolorization of synthetic dyes, Bioinorg. Chem. Appl. 2012 (2012).
[73] M.A. Yassin, A.A.M. Gad, Decolorization of dye effluents via immobilized glycoprotein peroxidase on post-consumer polystyrene foam, Int. J. Biol. Macromol. 236 (March) (2023) 124019, https://doi.org/10.1016/j.ijbiomac.2023.124019.
[74] L. Chen, M. Zou, F.F. Hong, Evaluation of fungal laccase immobilized on natural nanostructured bacterial cellulose, Front. Microbiol. 6 (Nov) (2015) 1–10.
[75] D. Yinghui, W. Qiuling, F. Shiyu, Laccase stabilization by covalent binding immobilization on activated polyvinyl alcohol carrier, Lett. Appl. Microbiol. 35 (6) (2002) 451–456.
[76] A. Nestorson, K.G. Neon, E.T. Kang, L. Järnström, A. Leufvén, Enzyme immobilization in latex dispersion coatings for active food packaging, Packag. Technol. Sci. 21 (4) (2008) 193–205.